

STABILITY OF THE MAGNETOPAUSE OF DISK-ACCRETING ROTATING STARS

R.V.E. LOVELACE¹, L. TURNER², AND M.M. ROMANOVA²*Draft version October 26, 2018*

ABSTRACT

We discuss three modes of oscillation of accretion disks around rotating magnetized neutron stars which may explain the separations of the kilo-Hertz -periodic oscillations (QPO) seen in low mass X-ray binaries. The existence of these compressible, non-barotropic magnetohydrodynamic (MHD) modes requires that there be a maximum in the angular velocity $\Omega_\phi(r)$ of the accreting material larger than the angular velocity of the star Ω_* , and that the fluid is in approximately circular motion near this maximum rather than moving rapidly towards the star or out of the disk plane into funnel flows. Our MHD simulations show this type of flow and $\Omega_\phi(r)$ profile. The first mode is a Rossby wave instability (RWI) mode which is radially trapped in the vicinity of the maximum of a key function $g(r)\mathcal{F}(r)$ at r_R . The real part of the angular frequency of the mode is $\omega_r = m\Omega_\phi(r_R)$, where $m = 1, 2, \dots$ is the azimuthal mode number. The second mode, is a mode driven by the rotating, non-axisymmetric component of the star's magnetic field. It has an angular frequency equal to the star's angular rotation rate Ω_* . This mode is strongly excited near the radius of the Lindblad resonance which is slightly outside of r_R . The third mode arises naturally from the interaction of flow perturbation with the rotating non-axisymmetric component of the star's magnetic field. It has an angular frequency $\Omega_*/2$. We suggest that the first mode with $m = 1$ is associated with the upper QPO frequency, ν_u ; that the nonlinear interaction of the first and second modes gives the lower QPO frequency, $\nu_\ell = \nu_u - \nu_*$; and that the nonlinear interaction of the first and third modes gives the lower QPO frequency $\nu_\ell = \nu_u - \nu_*/2$, where $\nu_* = \Omega_*/2\pi$.

Subject headings: keywords: accretion, accretion disks — stars: neutron — X-rays: binaries — magnetohydrodynamics — Instabilities — Waves

1. INTRODUCTION

Low mass X-ray binaries often display twin kilo-Hertz quasi-periodic oscillations (QPOs) in their X-ray emissions (van der Klis 2006; Zhang et al. 2006). A wide variety of different models have been proposed to explain the origin and correlations of the different QPOs. These include the beat frequency model (Miller, Lamb, & Psaltis 1998; Lamb & Miller 2001; Lamb & Miller 2003), the relativistic precession model (Stella & Vietri 1999), the Alfvén wave model (Zhang 2004), and warped disk models (Shirakawa & Lai 2002; Kato 2004).

A puzzling aspect of the some of the twin QPO sources considered in this work is that the difference between the upper ν_u and lower ν_ℓ QPO frequencies is roughly either the spin frequency of the star ν_* (3 cases where $\nu_* = 270, 330, \& 363$ Hz) or one-half this frequency, $\nu_*/2$ (4 cases where $\nu_* = 401, 524, 581, \& 619$ Hz), for the cases where ν_* is known, even though ν_u and ν_ℓ vary significantly (see, e.g., Zhang et al. 2006). A further type of behavior appears in the source Cir X-1 (Boutloukos et al. 2006), but this is not considered here. The cases where $\nu_u - \nu_\ell \approx \nu_*$ may be explained by the beat frequency model (Miller et al. 1998), but the explanation of the cases where $\nu_u - \nu_\ell \approx \nu_*/2$ is obscure.

Li and Narayan (2004) analyzed the stability of an incompressible rotating flow where the radial profiles of the plasma angular rotation rate Ω_ϕ , the magnetic field B_z , and the density ρ change sharply at the magnetopause radius but are independent of z . The magnetic field was dynamically important in the sense that $\rho\mathbf{u}^2 \sim \mathbf{B}^2/4\pi$ with $\mathbf{u} = r\Omega_\phi\hat{\phi}$. They found Rayleigh-Taylor and Kelvin-

Helmholtz type instabilities in the vicinity of the magnetopause. Recently, Fu and Lai (2009) have done a systematic analysis of short wavelength modes of a disk for cases where the magnetic field is not dynamically important.

The present work is a continuation of the study of Lovelace and Romanova (2007; hereafter LR07) of the magnetohydrodynamic (MHD) stability of the compressible, non-barotropic stability of the boundary between an accretion disk and the magnetosphere of a rotating magnetized star for conditions where Ω_ϕ , B_z , and ρ vary smoothly with radial distance but are independent of z , and where the magnetic field is dynamically important. The radial profiles of these quantities are known for different conditions from MHD simulations (Romanova et al. 2002; Long, Romanova, & Lovelace 2005; Romanova, Kulkarni, & Lovelace 2008; Kulkarni & Romanova 2008). The recent MHD studies (Romanova et al. 2008; Kulkarni & Romanova 2008) discovered conditions where a global Rayleigh-Taylor instability occurs and changes the nature of the accretion flow from a regular funnel flow pattern to a chaotic flow of plasma fingers. The present work is concerned with a radially localized instability of a globally stable approximately axisymmetric flow. Of particular importance to the present work is that $\Omega_\phi(r)$ is observed to go through a maximum significantly larger than the angular rotation rate of the star $\Omega_* = 2\pi\nu_*$. The importance of the maximum of $\Omega_\phi(r)$ for models of QPOs was discussed earlier by Alpar and Psaltis (2005). LR07 showed that there was a Rossby wave instability (RWI) or unstable corotation mode with azimuthal mode number $m = 1, 2, \dots$ radially trapped at r_R near the maximum of $\Omega_\phi(r)$. It was sug-

¹ Departments of Astronomy and Applied and Engineering Physics, Cornell University, Ithaca, NY 14853-6801; RVL1@cornell.edu

² Department of Astronomy, Cornell University, Ithaca, NY 14853-6801; turner@cornell.edu; romanova@astro.cornell.edu

gested that the upper QPO frequency was $\omega_r = m\Omega_\phi(r_R)$ and that the lower QPO frequency was due to the interaction of the mode with rotating non-axisymmetric field of the star. The theory of the RWI was developed by Lovelace et al. (1999) and Li et al. (2000) for accretion disks and earlier by Lovelace & Hohlfield (1978) for disk galaxies. Hydrodynamic simulations of the RWI instability in disks were done by Li et al. (2001), while Sellwood & Kahn (1991) used N -body simulations to study the instability in galaxies. The instability has important role in the accretion-ejection instability of disks discussed by Tagger and collaborators (e.g., Tagger & Varnière 2006; Tagger & Pellat 1999).

Section 2.1 develops the general compressible, non-barotropic MHD equations for *free* perturbations an axisymmetric equilibrium flow with no z -dependence. Section 2.2 treats the *driven* perturbations due to the rotating non-axisymmetric component of the star's magnetic field. Section 2.3 treats the *driven-modulated* perturbations which result from the interaction of the non-axisymmetric field of the star *and* the flow perturbation. Section 3 develops a detailed model of the axisymmetric flow/field equilibrium based on results from MHD simulations. Section 4 discusses the results obtained applying the theory of §2 to the model of §3. Section 4.1 treats the free perturbations, §4.2 the driven perturbations, and §4.3 the driven-modulated perturbations. Section 5 briefly discusses the nonlinear effect of the unstable mode. Section 6 gives the conclusions of this work.

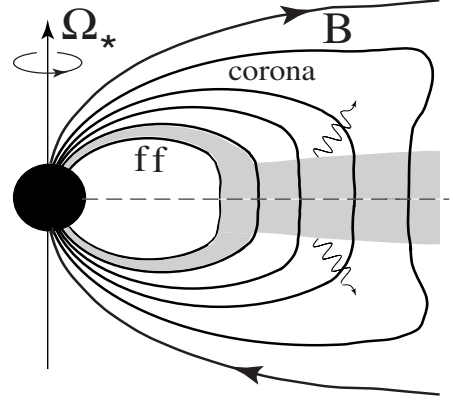


FIG. 1.— Sketch of the envisioned disk, magnetic field, and rotating star geometry. Ω_* is the angular rotation rate of the star, the wiggly lines indicates radiation from the surface of the disk where the optical depth is unity, and ff indicates the funnel flow. The region outside the disk and funnel flow is occupied by a low-density, high-temperature corona.

2.1. Free Perturbations

The perturbed quantities are: the density, $\tilde{\rho} = \rho + \delta\rho(r, \phi, t)$; the pressure is $\tilde{p} = p + \delta p(r, \phi, t)$; and the flow velocity is $\tilde{\mathbf{u}} = \mathbf{u} + \delta\mathbf{u}(r, \phi, t)$ with $\delta\mathbf{u} = (\delta u_r, \delta u_\phi, 0)$. Also, $\tilde{\mathbf{B}} = \hat{\mathbf{z}}B + \hat{\mathbf{z}}\delta B$. The equations for the perturbed flow are

$$\frac{D\tilde{\rho}}{Dt} + \tilde{\rho} \nabla \cdot \tilde{\mathbf{u}} = 0, \quad (1a)$$

$$\frac{D\tilde{\mathbf{u}}}{Dt} = -\frac{1}{\tilde{\rho}} \nabla \left(\tilde{p} + \frac{B^2}{8\pi} \right) - \nabla \Phi, \quad (1b)$$

$$\frac{DS}{Dt} = 0, \quad (1c)$$

$$\frac{D}{Dt} \left(\frac{B}{\rho} \right) = 0, \quad (1d)$$

$$\nabla^2 \Phi = 4\pi G\rho,$$

where $D/Dt \equiv \partial/\partial t + \tilde{\mathbf{u}} \cdot \nabla$ and we refer to $S \equiv \tilde{p}/(\tilde{\rho})^\gamma$ as the entropy of the disk matter.

We consider perturbations $\sim f(r)\exp(im\phi - i\omega t)$, where $m = 0, 1, 2, \dots$ is the azimuthal mode number and ω the angular frequency. For free perturbations $\omega = \omega_r + i\omega_i$ and for the growing modes of interest $\omega_i > 0$. (For the driven perturbations considered in §2.2 and 2.3, $\omega_i = 0$.) From equation (1a), we have

$$i\Delta\omega \delta\rho = \nabla \cdot (\rho \delta\mathbf{u}), \quad (2)$$

where $\Delta\omega(r) \equiv \omega - m\Omega_\phi(r)$ and $\Omega_\phi = u_\phi/r$.

From equation (1b) we have

$$i\Delta\omega \delta u_r + 2\Omega_\phi \delta u_\phi = \frac{1}{\rho} \frac{\partial \delta p_*}{\partial r} - \frac{\delta\rho}{\rho^2} \frac{dp_*}{dr} + \frac{\partial \delta \Phi}{\partial r}, \quad (3a)$$

$$i\Delta\omega \delta u_\phi - \frac{\Omega_r^2}{2\Omega_\phi} \delta u_r = ik_\phi \frac{\delta p_*}{\rho} + ik_\phi \delta \Phi. \quad (3b)$$

Here, $\Omega_r \equiv [r^{-3}d(r^4\Omega_\phi^2)/dr]^{1/2}$ is the radial epicyclic frequency, $k_\phi \equiv m/r$ is the azimuthal wavenumber,

$$p_* \equiv p + \frac{B^2}{8\pi}, \quad \text{and} \quad \delta p_* \equiv \delta p + \frac{B\delta B}{4\pi}.$$

From equation (1c) and (1d), we have

$$\delta p = c_s^2 \delta \rho - \frac{i \rho c_s^2}{\Delta \omega L_S} \delta u_r, \quad \text{and} \quad \delta B = \frac{\delta \rho}{\rho} B - \frac{i \rho \delta u_r}{\Delta \omega} \frac{d}{dr} \left(\frac{B}{\rho} \right).$$

Combining these expressions,

$$\delta p_* = (c_s^2 + c_A^2) \delta \rho - \frac{i \rho \delta u_r}{\Delta \omega} \left(\frac{c_s^2}{L_S} + \frac{c_A^2}{L_B} \right), \quad (4)$$

where

$$\frac{1}{L_S} \equiv \frac{1}{\gamma} \frac{d \ln(S)}{dr}, \quad \frac{1}{L_B} \equiv \frac{d \ln(B/\rho)}{dr}, \quad (5a)$$

are the length-scales of the entropy $S \equiv p/\rho^\gamma$ and B/ρ variations. Also,

$$c_s \equiv \left(\frac{\gamma p}{\rho} \right)^{1/2}, \quad \text{and} \quad c_A = \frac{|B|}{\sqrt{4\pi\rho}}, \quad (5b)$$

are the sound and Alfvén speeds respectively. We denote $c_f \equiv (c_s^2 + c_A^2)^{1/2}$ as the fast magnetosonic speed.

It is useful to introduce

$$\Psi \equiv \frac{\delta p_*}{\rho}. \quad (6)$$

Equations (3) can then be written as

$$A \delta u_r + B \delta u_\phi = f_r, \quad (7a)$$

$$C \delta u_\phi + D \delta u_r = f_\phi, \quad (7b)$$

where

$$A = -i \left[\Delta \omega + \frac{dp_*/dr}{\Delta \omega \rho L_*} \right],$$

$$B = -2\Omega_\phi, \quad C = -i\Delta\omega, \quad D = \frac{\Omega_r^2}{2\Omega_\phi}.$$

Also,

$$f_r = -\frac{\partial \Psi}{\partial r} + \frac{\Psi}{L_*} - \frac{\partial \delta \Phi}{\partial r},$$

$$f_\phi = -ik_\phi(\Psi + \delta \Phi),$$

where

$$\frac{1}{L_*} \equiv \frac{1}{\rho c_f^2} \frac{dp_*}{dr} - \frac{1}{L_\rho} = \frac{1}{c_f^2} \left(\frac{c_s^2}{L_S} + \frac{c_A^2}{L_B} \right), \quad (8a)$$

and where

$$\frac{1}{L_\rho} \equiv \frac{d \ln(\rho)}{dr}. \quad (8b)$$

For a strong magnetic field $c_A \gg c_s$ we have $L_* \rightarrow L_B$. For a weak magnetic field $c_A \ll c_s$, we have $L_* \rightarrow L_S$. Using the equation for the equilibrium $\rho r(\Omega_K^2 - \Omega_\phi^2) = -dp_*/dr$ we have

$$\frac{1}{L_*} = -\frac{r(\Omega_K^2 - \Omega_\phi^2)}{c_f^2} - \frac{1}{L_\rho}, \quad (8c)$$

which is useful later.

From here on we simplify the analysis by neglecting the self-gravity of the disk. That is, we neglect the $\delta \Phi$ terms in f_r and f_ϕ .

We solve equations (7a) and (7b) to obtain

$$\rho \delta u_r = i\mathcal{F} \left[\frac{\Delta \omega}{\Omega_\phi} \left(\frac{\partial \Psi}{\partial r} - \frac{\Psi}{L_*} \right) - 2k_\phi \Psi \right], \quad (9a)$$

$$\rho \delta u_\phi = \mathcal{F} \left\{ \frac{\Omega_r^2}{2\Omega_\phi^2} \left(\frac{\partial \Psi}{\partial r} - \frac{\Psi}{L_*} \right) \right.$$

$$\left. - k_\phi \left(\frac{\Delta \omega}{\Omega_\phi} + \frac{dp_*/dr}{\rho \Omega_\phi \Delta \omega L_*} \right) \Psi \right\}. \quad (9b)$$

Here,

$$\mathcal{F} \equiv \frac{\rho \Omega_\phi}{\mathcal{D}}, \quad (10a)$$

where

$$\mathcal{D} = \Omega_r^2 - (\Delta \omega)^2 - \frac{dp_*/dr}{\rho L_*}, \quad (10b)$$

is the ‘Lindblad factor.’ For real frequencies ω , $\mathcal{D}(r)$ is equal to zero at a Lindblad resonance at r_L . On the other hand at a corotation resonance $\Re[\Delta \omega(r)] = 0$ at r_R . Using equation (8c) we find

$$\mathcal{D} = \Omega_r^2 - (\Delta \omega)^2 - \frac{r^2(\Omega_K^2 - \Omega_\phi^2)^2}{c_f^2} - \frac{r(\Omega_K^2 - \Omega_\phi^2)}{L_\rho}. \quad (10c)$$

Equations (9) can now be used to obtain

$$\begin{aligned} \nabla \cdot (\rho \delta \mathbf{v}) &= \overbrace{\frac{i \Delta \omega}{r} \frac{\partial}{\partial r} \left(\frac{r \mathcal{F}}{\Omega_\phi} \frac{\partial \Psi}{\partial r} \right)} + \frac{i \mathcal{F}}{\Omega_\phi} \frac{\partial \Delta \omega}{\partial r} \frac{\partial \Psi}{\partial r} \\ &- \frac{i}{r} \left[\frac{\partial}{\partial r} \left(\frac{r \mathcal{F} \Delta \omega}{\Omega_\phi L_*} \right) \right] \Psi - \frac{i \mathcal{F} \Delta \omega}{\Omega_\phi L_*} \frac{\partial \Psi}{\partial r} - 2ik_\phi \frac{\partial \mathcal{F}}{\partial r} \Psi \\ &- 2ik_\phi \mathcal{F} \frac{\partial \Psi}{\partial r} - \frac{ik_\phi \mathcal{F} \Omega_r^2}{2\Omega_\phi^2 L_*} \Psi + \frac{ik_\phi \mathcal{F} \Omega_r^2}{2\Omega_\phi^2} \frac{\partial \Psi}{\partial r} \\ &- ik_\phi^2 \mathcal{F} \left[\frac{\Delta \omega}{\Omega_\phi} + \frac{dp_*/dr}{\rho \Omega_\phi \Delta \omega L_*} \right] \Psi. \end{aligned} \quad (11)$$

It is useful to note that

$$\frac{\partial \Delta \omega}{\partial r} = -\frac{k_\phi(\Omega_r^2 - 4\Omega_\phi^2)}{2\Omega_\phi}.$$

From equations (4) and (9a) we have

$$\delta \rho = \frac{\rho \Psi}{c_f^2} - \frac{\mathcal{F}}{\Delta \omega L_*} \left[\frac{\Delta \omega}{\Omega_\phi} \left(\frac{\partial \Psi}{\partial r} - \frac{\Psi}{L_*} \right) - 2k_\phi \Psi \right]. \quad (12)$$

Equations (11) and (12) can now be substituted into equation (2). When this is done we find that all of the terms involving $\partial \Psi / \partial r$ apart from the overbraced term in equation (11) cancel out.

Combining equations (9) with equation (2) gives

$$\begin{aligned} &\frac{1}{r} \frac{\partial}{\partial r} \left(\frac{r \mathcal{F}}{\Omega_\phi} \frac{\partial \Psi}{\partial r} \right) = \\ &\left[\frac{\rho}{c_f^2} + \frac{k_\phi^2 \mathcal{F}}{\Omega_\phi} + \frac{1}{r} \frac{\partial}{\partial r} \left(\frac{r \mathcal{F}}{\Omega_\phi L_*} \right) + \frac{\mathcal{F}}{\Omega_\phi L_*^2} \right] \Psi \\ &+ \left[2k_\phi \mathcal{F} \frac{d \ln(g \mathcal{F})}{dr} \right] \frac{\Psi}{\Delta \omega} + \left[\frac{k_\phi^2 (dp_*/dr) \mathcal{F}}{\rho \Omega_\phi L_*} \right] \frac{\Psi}{(\Delta \omega)^2}, \end{aligned} \quad (13)$$

where $g = \exp(2 \int dr/L_*)$. In the limit of no magnetic field ($c_A \rightarrow 0$ and $L_* \rightarrow L_S$), this equation becomes the same as the equation for the Rossby wave instability (Lovelace et al. 1999; Li et al. 2000).

A quadratic form can be obtained by multiplying equation (13) by Ψ^* (the complex conjugate of Ψ) and integrating over the disk. Assuming $r \Psi^* (d\Psi/dr) \mathcal{F} / \Omega_\phi \rightarrow 0$ for $r \rightarrow 0, \infty$, we obtain

$$- \int d^2 r \frac{\mathcal{F}}{\Omega_\phi} \left(\left| \frac{\partial \Psi}{\partial r} \right|^2 + k_\phi^2 |\Psi|^2 \right) = \int d^2 r \frac{\rho}{c_f^2} |\Psi|^2$$

$$\begin{aligned}
& + \int d^2r \left[\frac{1}{r} \frac{\partial}{\partial r} \left(\frac{r\mathcal{F}}{\Omega_\phi L_*} \right) + \frac{\mathcal{F}}{\Omega_\phi L_*^2} \right] |\Psi|^2 \\
& + 2 \int d^2r k_\phi \mathcal{F} \frac{d \ln(g\mathcal{F})}{dr} \frac{|\Psi|^2}{\Delta\omega} \\
& + \int d^2r \frac{k_\phi^2 (dp_*/dr) \mathcal{F}}{\rho \Omega_\phi L_*} \frac{|\Psi|^2}{(\Delta\omega)^2}. \quad (14)
\end{aligned}$$

For corotation modes where $|\Delta\omega|^2 \ll \Omega_\phi^2$, the third and fourth integrals on the right-hand side of equation (14) are possibly important. Earlier work by Lovelace and Hohlfield (1978), Lovelace et al. (1999), and Li et al. (2000) found that a corotation instability was possible if the quantity $g\mathcal{F}$ has a maximum or minimum at the radial distance r_R where $\Re(\Delta\omega) = 0$. For a weak magnetic field ($c_A^2 \ll c_s^2$ where $L_* \approx L_S$), we find $g\mathcal{F} = S^{2/\gamma} \mathcal{F}$ which agrees with the result of Lovelace et al. (1999) and Li et al. (2000) where the self-gravity of the disk was neglected. With negligible self-gravity, instability is found only for conditions where $g\mathcal{F}$ has a *maximum* as a function of r . For a maximum the radial group velocity of the Rossby waves is directed towards r_R (Lovelace et al. 1999). In the strong B -field limit ($c_A^2 \gg c_s^2$ where $L_* \approx L_B$), $g\mathcal{F} = (B/\rho)^2 \mathcal{F}$.

We can rewrite equation (13) in a form more amenable to numerical analysis. That is,

$$\Psi'' = \left(\frac{\overline{\mathcal{D}'}}{\overline{\mathcal{D}}} \right) \Psi' + \left(C_0 + \frac{C_1}{\Delta\omega} + \frac{C_2}{(\Delta\omega)^2} \right) \Psi, \quad (15)$$

where $\overline{\mathcal{D}} \equiv \mathcal{D}/(r\rho) = (\Omega_\phi/r)\mathcal{F}^{-1}$, where \mathcal{D} is given by equation (10b), and \mathcal{F} by equation (10a). The primes denote radial derivatives. Also,

$$\begin{aligned}
C_0 &= k_\phi^2 + \frac{\mathcal{D}}{c_f^2} - \frac{\overline{\mathcal{D}'}}{L_* \overline{\mathcal{D}}} + \frac{1 - L_*'}{L_*^2}, \\
C_1 &= 2k_\phi \Omega_\phi [\ln(g\mathcal{F})]', \quad C_2 = k_\phi^2 \frac{p_*'}{\rho L_*}, \quad (16)
\end{aligned}$$

where g is defined below equation (13).

If we let $\Psi = (\overline{\mathcal{D}})^{1/2} \varphi$, then equation (15) can be written in the form of a Schrödinger equation,

$$\begin{aligned}
\varphi'' &= \left(\overline{\mathcal{C}}_0 + \frac{C_1}{\Delta\omega} + \frac{C_2}{(\Delta\omega)^2} \right) \varphi \equiv U(r)\varphi, \\
\overline{\mathcal{C}}_0 &\equiv C_0 + \frac{3}{4} \left(\frac{\overline{\mathcal{D}'}}{\overline{\mathcal{D}}} \right)^2 - \frac{1}{2} \left(\frac{\overline{\mathcal{D}''}}{\overline{\mathcal{D}}} \right), \quad (17)
\end{aligned}$$

where $U(r)$ is an effective potential. Both U and φ are in general complex for complex ω .

A quadratic form analogous to equation (14) can be obtained by multiplying equation (17) by $\varphi^* dr$ and integrating over r . Assuming $\varphi^* \varphi'$ vanishes at small and large r , we obtain

$$\begin{aligned}
- \int dr |\varphi'|^2 &= \int dr \overline{\mathcal{C}}_0 |\varphi|^2 + 2 \int dr k_\phi \Omega_\phi \frac{[\ln(g\mathcal{F})]'}{\Delta\omega} |\varphi|^2 \\
&+ \int dr \frac{C_2}{(\Delta\omega)^2} |\varphi|^2. \quad (18)
\end{aligned}$$

The imaginary part of this equation gives

$$0 = \dots - \omega_i \int dr \frac{[\ln(g\mathcal{F})]'}{(\Delta\omega_r)^2 + \omega_i^2} |\varphi|^2 + \dots, \quad (19)$$

where the ellipsis allow for contributions from the $\overline{\mathcal{C}}_0$ and C_2 terms. If these terms are negligible as found in our numerical evaluations, it follows that a non-zero growth rate ω_i is possible only for conditions where $[\ln(g\mathcal{F})]'$ changes sign as mention above (Lovelace & Hohlfield 1978). Thus, $g\mathcal{F}$ is a key function for stability of the considered flow.

Using equations (4), (9a), and (12) we obtain the relation of the temperature perturbation to Ψ ,

$$\begin{aligned}
\frac{\delta T}{T} &= A_0 \Psi + A_1 \Psi', \\
A_0 &= \frac{\gamma - 1}{c_f^2} + \frac{1}{\mathcal{D}} \left(\frac{\gamma - 1}{L_*^2} - \frac{\gamma}{L_S^2} \right) + \frac{2k_\phi \Omega_\phi}{\mathcal{D} \Delta\omega} \left(\frac{\gamma - 1}{L_*} - \frac{\gamma}{L_S} \right), \\
A_1 &= \frac{1}{\mathcal{D}} \left(\frac{\gamma}{L_S} - \frac{\gamma - 1}{L_*} \right). \quad (20)
\end{aligned}$$

This equation shows that the temperature perturbation is strongly enhanced at a corotation resonance where $|\Delta\omega|$ becomes very small and at a Lindblad resonance where $\mathcal{D} = 0$.

2.2. Driven Perturbations

The influence of a small non-axisymmetric component of the stellar magnetic field can be studied by including in equation (1b) the small force due to this non-axisymmetry. At a given radial distance, the total vertical magnetic field $B = B^v + B^i$ consists of the vacuum component B^v due to current flow inside the star and the induced field B^i due to the current flow in the plasma outside the star. The vacuum field has the general form

$$\begin{aligned}
B^v &= B^{v0}(r) + \Delta B^v(r, \phi, t), \\
\Delta B^v &= B^{v1}(r) \exp(i\phi - i\Omega_* t) + B^{v2}(r) \exp(2i\phi - i\Omega_* t) + \dots, \quad (21)
\end{aligned}$$

where B^{v0} is the axisymmetric component, $B^{v1} \ll B^{v0}$ is the quadrupole component, and $B^{v2} \ll B^{v0}$ is the octupole component. The quadrupole term can represent a non-centered but aligned dipole field in the star. The total magnetic force or acceleration is $\mathbf{F} = -\nabla \{ \langle B \rangle + \Delta B^v \} / (8\pi\rho)$, (because $(\mathbf{B} \cdot \nabla) \mathbf{B} = 0$), where $\langle B \rangle = \langle B^i + B^v \rangle$ and where the average is over ϕ . Linearization gives $\delta \mathbf{F} = -\nabla [\langle B \rangle \Delta B^v(r, \phi, t)] / (4\pi\rho)$. Thus we have

$$(\delta F_r, \delta F_\phi) = (\delta F_{r0}, \delta F_{\phi0}) \exp(im\phi - i\Omega_* t), \quad (22)$$

where $m = 1$ or 2 and Ω_* is the angular rotation rate of the star. The calculation of §2.1 is modified slightly beginning with equations (7) which are here replaced by

$$\begin{aligned}
A\delta v_r + B\delta v_\phi &= f_r + \delta F_r, \\
C\delta v_\phi + D\delta v_r &= f_\phi + \delta F_\phi, \quad (23)
\end{aligned}$$

where A, \dots, D are the same as defined below equation (7).

The forcing term $\delta \mathbf{F}$ gives rise to an additional contribution to $\rho \delta \mathbf{v}$ not included in §2.1. This contribution is

$$\begin{aligned}
\rho \delta v_r &= \frac{1}{r\overline{\mathcal{D}}} (-C\delta F_r + B\delta F_\phi) \equiv H_r, \\
\rho \delta v_\phi &= \frac{1}{r\overline{\mathcal{D}}} (D\delta F_r - A\delta F_\phi) \equiv H_\phi, \quad (24)
\end{aligned}$$

where $\overline{\mathcal{D}} = \mathcal{D}/(r\rho)$ and \mathcal{D} is the Lindblad factor defined in equation (10b). Including this contribution we find that response of the flow $\varphi = \Psi/(\overline{\mathcal{D}})^{1/2}$ is given by

$$\varphi'' - U(r)\varphi = i \frac{r(\overline{\mathcal{D}})^{1/2}}{\Delta\omega} \nabla \cdot \mathbf{H}, \quad (25)$$

where U is defined in equation (17) and \mathbf{H} is a known function determined by ΔB^v . We are interested in only the inhomogeneous solutions to this equation where U , ω , $\Delta\omega$, and $\overline{\mathcal{D}}$ are real.

2.3. Driven-Modulated Perturbations

Here we consider the case where the abovementioned driving force $\delta\mathbf{F}$ is modulated by the flow perturbation Ψ (LR07). This modulation comes about naturally by including the magnetic field perturbation δB in the magnetic force \mathbf{F} . That is, $\mathbf{F} = -\nabla\{[\langle B \rangle + \delta B + \Delta B^v]^2\}/(8\pi\rho)$. Linearization of this force gives a contribution $\mathbf{F}^m = -\nabla[\delta B \Delta B^v]/(4\pi\rho)$. The equations of §2.1 can be used to derive an exact formula relating δB to Ψ , but here we use a simplified formula for one of the dominant terms, $\delta B = B\Psi(\mathcal{D}L_*^2)^{-1}$, in order to limit the complexity of the equations. An equation for the driven modulated perturbations is then obtained by the replacement in equation (23) of $\delta\mathbf{F} \rightarrow \delta\mathbf{F}^m = \Psi^*\delta\mathbf{F}/(\mathcal{D}L_*^2)$, where $\delta\mathbf{F}$ is still given by equation (22) and is a known function determined by ΔB^v . The use of Ψ^* rather than Ψ is required due to our assumed dependence of $\delta\mathbf{F}$ in equation (22). For the driven-modulated perturbations we obtain in place of equation (25)

$$\varphi'' - \widehat{U}(r)\varphi = i \frac{r(\widehat{\mathcal{D}})^{1/2}}{\Delta\omega} \nabla \cdot \left\{ \widehat{\mathbf{M}} \cdot \left[\left(\frac{\widehat{\mathcal{D}}^{-1/2}}{r\rho L_*^2} \varphi \right)^* \delta\mathbf{F} \right] \right\}, \quad (26)$$

where we have used the fact that $\Psi = (\overline{\mathcal{D}})^{1/2}\varphi$. The hats over different quantities indicates that they are now operators with $\omega \rightarrow i(\partial/\partial t)$ and $k_\phi \rightarrow -i(\partial/\partial\phi)$. The matrix \mathbf{M} allows us to write equation (24) as $\mathbf{H} = \mathbf{M} \cdot \delta\mathbf{F}$.

Equation (26) is a linear equation for φ so that in general

$$\varphi = \varphi_0 \exp(-i\omega t) + \varphi_1 \exp(i\phi - i\omega t) + \varphi_2 \exp(2i\phi - i\omega t) + \dots, \quad (27)$$

where ω is real but undetermined at this point. Clearly, the time and angle dependence on both sides of equation (26) must match.

For the case where there is a small quadrupole field component $\Delta B = B^{v1} \exp(i\phi - i\omega t)$, equation (26) implies

$$\begin{aligned} \varphi_0'' - U_{0,\omega}(r)\varphi_0 &= [\text{Op}(\varphi_1^*)]_{0,\omega} \quad (m=0), \\ \varphi_1'' - U_{1,\omega}(r)\varphi_1 &= [\text{Op}(\varphi_0^*)]_{1,\omega} \quad (m=1), \end{aligned} \quad (28)$$

where Op stands for the linear operator on φ^* on the right-hand side of equation (26) and the new subscripts indicate the m value and the ω value. Here, we necessarily have

$$\omega = \frac{\Omega_*}{2}, \quad (29)$$

as found earlier by LR07.

For the case where there is a small octupole field component $\Delta B = B^{v2} \exp(2i\phi - i\omega t)$, equation (26) implies

$$\varphi_1'' - U_{1,\omega}(r)\varphi_1 = [\text{Op}(\varphi_1^*)]_{1,\omega}, \quad (30)$$

where we again have $\omega = \Omega_*/2$.

In contrast with the case of driven perturbations of §2.2, equation (26) is linear in φ so that its magnitude is indeterminate. Further study is needed to determine the magnitude of φ in this case. One possibility is to generalize equation (26) to include on the right-hand-side of the equation the inhomogeneous driving force $\propto \delta\mathbf{F}$ as

well the nonlinear force $\delta\mathbf{F}^{nl} = -\nabla(|\delta B|^2)/(8\pi\rho)$. Owing to the nonlinearity the driving force $\delta\mathbf{F}$ at frequency Ω_* can generate the 1/2 subharmonic oscillations of φ at the frequency $\Omega_*/2$ described by equation (26). Analogous subharmonic generation is known in similar systems (e.g., Minorsky 1974).

3. MODEL OF EQUILIBRIUM

Figure 2 shows sample measured profiles of the midplane axial magnetic field (B), the azimuthal frequency of the disk matter [$\nu_\phi = v_\phi/(2\pi r)$] and its density (ρ) from MHD simulations by Romanova, Kulkarni, & Lovelace (2008) for globally stable case. The simulations were three dimensional for an approximately axisymmetric case. These profiles motivate our choice of analytic functions to represent these quantities.

The fact that $\nu_\phi(r)$ decreases as r decreases close to the star is due to magnetic braking. A small twist of the star's magnetic field transports angular momentum of the disk matter to the star. That is, for $z > 0$ there is a vertical flux of angular momentum $-rB_\phi B_z/(4\pi) > 0$ with $|B_\phi| \ll |B_z|$ which transports the disk angular momentum to the star along the star's field lines (see Figure 1). This loss of angular momentum implies a mass accretion rate of the disk (outside of the region of the funnel flow) of $\dot{M}_d = -r^2(B_\phi)_h B_z/(d\ell/dr)$ ($= \text{const}$) in the absence of viscosity (see Lovelace, Romanova, & Newman 1994), where the h -subscript indicates evaluation at the top surface of the disk, $\ell = ru_\phi$ is the specific angular momentum, and $d\ell/dr$ is positive for the considered profiles. The turbulent viscosity due to the magnetorotational instability (MRI) is absent in the region of the disk where $c_A > c_s$ and/or $d\Omega_\phi/dr > 0$ (Balbus & Hawley 1998). Note however that the disk equilibria discussed below neglect the accretion and have $B_\phi = 0$.

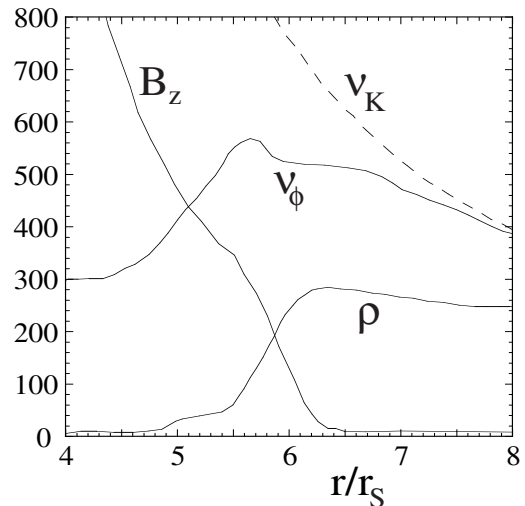


FIG. 2.— Midplane radial profiles of the magnetic field, the azimuthal frequency [$\nu_\phi = v_\phi/(2\pi r)$], the Keplerian frequency (ν_K), and the density ρ from the MHD simulations. The vertical scale is for the azimuthal frequency of the disk matter; the star's frequency is $\nu_* = 300$ Hz. The scalings of B_z and ρ is arbitrary.

We assume a pseudo-Newtonian gravitational potential $\Phi_g = -GM_*/(r - r_S)$, where M_* is the star's mass and $r_S \equiv 2GM_*/c^2 = 4.14 \times 10^5$ cm for a $1.4M_\odot$ star. The

angular velocity of a single pararticle is $\Omega_K = 2\pi\nu_K = \{GM_*/[r(r-r_S)^2]\}^{1/2}$ for $r \geq 3r_S$. Near the star, the rotation frequency of the matter is modeled following LR07 as

$$\nu_\phi^0(r) = \frac{\nu_* f(r)}{1+f(r)} + \frac{\nu_K(r)}{1+f(r)}, \quad (31)$$

which is a first approximation as explained below. Here, ν_* is the rotation frequency of the star and $f(r) \equiv \exp[-(r-r_0)/\Delta]$ with r_0 the standoff distance of the boundary layer and Δ is its thickness. The azimuthal velocity of the matter is $v_\phi = 2\pi r \nu_\phi^0$. Both r_0 and Δ are expected to depend on the accretion rate and the star's magnetic field.

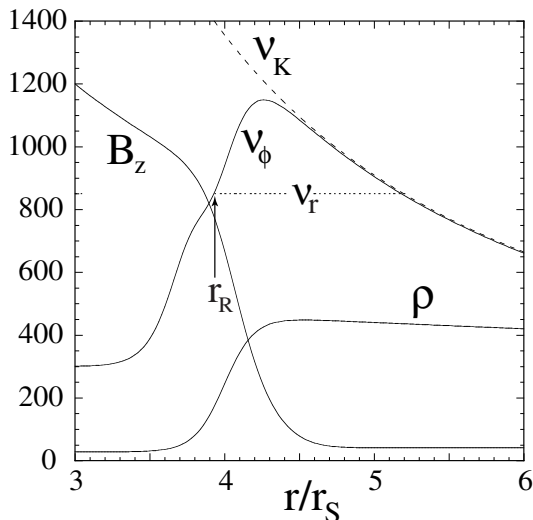


FIG. 3.— Radial profiles of the magnetic field (B_z), the azimuthal frequency [$\nu_\phi = v_\phi/(2\pi r)$], the Keplerian frequency (ν_K), and the density ρ of the model discussed in §3. The horizontal dotted line indicates the real part of the frequency ν_r of the unstable $m = 1$ corotation mode discussed in §4.1. The vertical scale is for the azimuthal frequency of the disk matter; the star's frequency is taken to be $\nu_* = 300$ Hz. The plot scales for B_z and ρ are arbitrary. For this case, $r_0/r_S = 4$ and $\Delta/r_S = 0.1$ in equation (25), $\epsilon = 0.05$ and $\rho_0 = 0.013$ g cm $^{-3}$ in equation (26), $\gamma = 5/3$, and at $r/r_S = 6$, $c_A/c_s = 0.156$. For this plot $B_z(r=r_0) = 9.32 \times 10^8$ G.

The radial force equilibrium for the axisymmetric flow is

$$\rho r (2\pi)^2 (\nu_K^2 - \nu_\phi^2) = - \frac{d}{dr} \left(p + \frac{B^2}{8\pi} \right), \quad (32)$$

where $p = \rho c_s^2/\gamma$ is the pressure in the disk and c_s is the sound speed. The density profile is modeled as

$$\rho = \rho_0 \left(\epsilon + \frac{(1-\epsilon) \exp(-0.05r/r_S)}{1+f(r)} \right), \quad (33)$$

with $f(r)$ the same function as in equation (31) and ϵ is a positive quantity much less than unity. The sound speed is modeled by choosing say $c_{sK} = 0.1r\Omega_K(r)$ and then letting

$$c_s = \frac{c_{sK}(r_0)f(r)}{1+f(r)} + \frac{c_{sK}(r)}{1+f(r)}. \quad (34)$$

At large distances $r \gg r_0$, $c_s/v_\phi = 0.1$ corresponds to a disk half-thickness $h \approx 0.1r$. Inside of r_0 the sound speed is assumed to be a constant. Using these expressions we first solve equation (32) for B^2 using equation (31) and neglecting the pressure gradient. We then go

back and obtain the correction $\delta\nu_\phi$ to the azimuthal frequency needed to account for the pressure gradient; that is, $2\rho r (2\pi)^2 \nu_\phi^0 \delta\nu_\phi = dp/dr$ so that the actual rotation frequency is $\nu_\phi = \nu_\phi^0 + \delta\nu_\phi$. The correction is small, $|\delta\nu_\phi/\nu_\phi^0| \sim (c_s/v_\phi)^2 \ll 1$. The radial epicyclic frequency is calculated from $\Omega_r = 2\pi\nu_r$ with $\nu_r^2 = r^{-3} d(r^4 \nu_\phi^2)/dr$.

Representative curves are shown in Figures 3 and 4. The value of the magnetic field at $r/r_S = 6$ is arbitrary, but here it is chosen so that $c_A < c_s$ which allows the MRI to grow which in turn gives rise to a turbulent viscosity in the disk (Balbus & Hawley 1998). The maximum of the disk frequency ν_ϕ is about $1149(4r_S/r_0)^{1.68}$ Hz for $\Delta/r_S = 0.1$, and it occurs at a distance about $0.26r_S$ larger than r_0 . For $\Delta/r_S = 0.2$, the maximum of ν_ϕ is somewhat smaller and it occurs at a distance about $0.4r_S$ larger than r_0 .

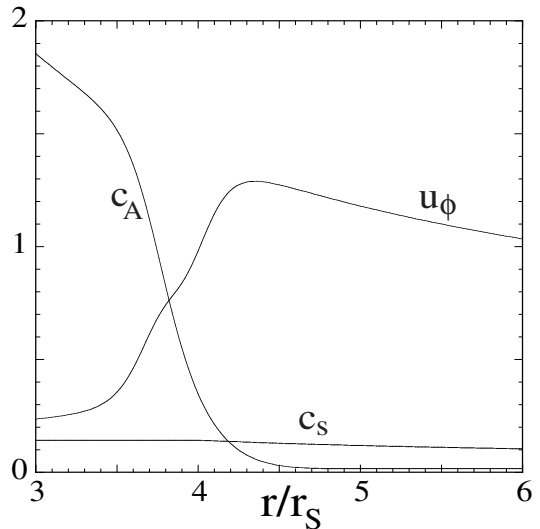


FIG. 4.— Radial dependences of the Alfvén speed, c_A , sound speed c_s , and azimuthal velocity u_ϕ for the same conditions as in Figure 3. In this plot the speeds are in units of 10^{10} cm/s.

4. RESULTS

We solve the equations of §2 using the equilibrium profiles of §3. For this we use Maple V. 12 where we define about 40 different functions of $R = r/r_S$, for example, $\rho(R)$, $\nu_\phi(R)$, $\nu_r(R)$, $\Delta\omega(R)$, $B(R)$, ..., $U(R)$. Some of the functions, for example, U , are complex for complex ω . The axisymmetric ($m = 0$) perturbation are found to be *stable* if the width of the boundary layer is not too narrow; that is, there is stability for $\Delta/r_S \gtrsim 0.02$. In the following we consider the possible instability of modes with $m = 1, 2, \dots$

4.1. Free Perturbations

Figure 5 shows the radial dependence of the real part of the key function $g(r)\mathcal{F}(r)$ for the same conditions as Figure 3. This function has a maximum at $r_R = 3.92r_S$ indicated by the vertical arrow marked corotation resonance. The function changes sign at $r_L = 4.07r_S$ which is a Lindblad resonance where \mathcal{F} (and \mathcal{D}) change signs. The maximum of $\Re[g(r)\mathcal{F}(r)]$ appears to be a general feature for profiles similar to those in Figure 2. The dependence can be traced to the dependence of $\mathcal{D}(r)$ (equation 10b). For r decreasing significantly below r_0 , the

term $-(dp_*/dr)/(\rho L_*)$ in \mathcal{D} becomes increasingly negative. This is due to the radial dependence of the magnetic pressure and the small density. Note L_* is negative in this region. On the other hand for r increasing from $\sim r_0$, the positive contribution of Ω_r^2 begins to dominate. The combination of these dependences gives a $\Re[g(r)\mathcal{F}(r)]$ profile with a maximum at a distance inside the Lindblad resonance as shown in Figure 5.

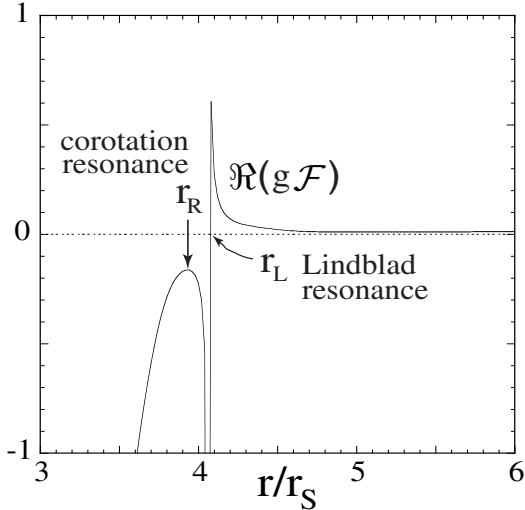


FIG. 5.— Radial dependence of the real part of the key function $g\mathcal{F}$ for the same conditions as for Figure 3. The imaginary part of the function is small compared with the real part. The function has only a weak dependence on ω which for this plot is $\omega \approx 850 + i89$ Hz. We find maximum instability for $\Re[\Delta\omega(r)] = 0$ at the radial location of the maximum of $\Re(g\mathcal{F})$ indicated by the vertical arrow. The other arrow shows a Lindblad resonance where $\Re(\mathcal{F})$ changes sign. The vertical scale is arbitrary.

Figure 6 shows the real part of the effective potential $U(r)$ for the same case as Figure 5. The real part of the frequency is chosen to give $\Re[\Delta\omega(r)] = 0$ at $r_R/r_S = 3.92$ of the maximum of $\Re[g(r)\mathcal{F}(r)]$ because this give the maximum growth rate. For $m = 1$ this gives $\nu_r = \omega_r/2\pi = 850$ Hz. Clearly this frequency must be larger than rotation frequency of the star ν_* .

The depth of the potential well shown in Figure 6 increases as the imaginary part of the frequency $\omega_i = \Im(\omega) > 0$ (the growth rate) decreases. We use a WKBJ treatment with $\varphi \propto k^{-1/2} \exp(\pm i \int^r dr k)$ and $k = [-\Re(U)]^{1/2}$. The imaginary part of U is small compared with the real part. The allowed values of ω_i are then calculated using the Bohr-Sommerfeld quantization condition,

$$\int_{r_{\text{in}}}^{r_{\text{out}}} dr k = \left(n + \frac{1}{2}\right) \pi, \quad n = 0, 1, 2, \dots, \quad (35)$$

where $k \equiv \sqrt{-\Re(U)}$, and r_{in} , & r_{out} are the radii where $\Re(U) = 0$.

For the case of Figure 6, $r_{\text{in}}/r_S = 3.83$ and $r_{\text{out}}/r_S = 3.97$. The largest growth rate ω_i corresponds to $n = 0$ and for the case of Figure 6 with $m = 1$ this gives $\nu_i = \omega_i/2\pi = 89$ Hz so that $\omega_i/\omega_r \approx 10\%$. For modes with $m \geq 2$ also grow with similar ω_i/ω_r values but as discussed below these modes do not give time variations in the total flux from the source.

For a more gradual boundary layer with $\Delta = 0.2$ and $m = 1$, we find $\Re[\Delta\omega(r)] = 0$ for $\nu_r = 750$ Hz at the ra-

dius $r/r_S = 3.83$ of the maximum of $\Re[g(r)\mathcal{F}(r)]$. From equation (35) we find $\nu_i = 120$ Hz. For Δ increasing from 0.2, we find that ν_r and r_R continue to decrease gradually and ν_i also decreases.

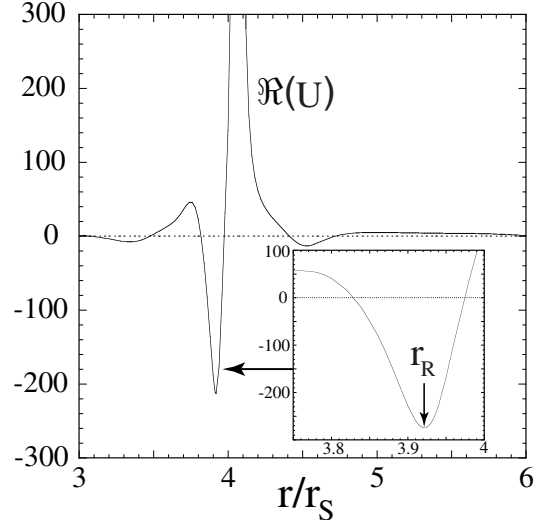


FIG. 6.— Radial dependence of the real part of the effective potential $\Re[U(r)]$ (multiplied by r_S^2) for the same conditions as for Figure 5. The imaginary part of U is much smaller than the real part.

Owing to the perturbation, the surface temperature of the disk is

$$T(r, \phi, t) = T_0 + \Re[\delta T_1 \exp(i\phi - i\omega_1 t) + \delta T_2(r) \exp(2i\phi - i\omega_2 t) + \dots], \quad (36)$$

where $T_0(r)$ is the unperturbed temperature, $\delta T_{1,2}(r) \ll T_0$ are the amplitudes of the $m = 1, 2$ corotation modes, and $\omega_{1,2}$ are their frequencies. We neglect the difference between the midplane and the surface temperature of the disk. The corresponding flux density from the disk surface is proportional to $S(r, \phi, t) \sim T_0^4 + \Re[4T_0^3 \delta T_1 \exp(i\phi - i\omega_1 t) + 4T_0^3 \delta T_2 \exp(2i\phi - i\omega_2 t) + \dots]$. The total flux for a face-on disk, $L \sim \int r dr d\phi S$, is independent of time: the ϕ -integration annihilates the terms dependent on ϕ . For a more general disk orientation, with the disk angular momentum tilted say towards the line of sight by an angle ι , the Doppler effect due to the disk rotation gives a boost to the frequency for say $\phi = 0$ and a decrement for $\phi = \pi$. This corresponds to multiplying S by the Doppler factor $D(r, \phi) \equiv [1 + \varepsilon(r) \cos(\phi)]^4 \approx 1 + 4\varepsilon \cos(\phi)$, where $\varepsilon = [v_\phi(r)/c] \sin(\iota)$ and $\varepsilon^2 \ll 1$. For the case of Figure 6 where $r = 3.92r_s$, $v_\phi/c = 0.289$. Consequently, there is a contribution to the source flux $\delta L \sim \int r dr d\phi D(r, \phi) S(r, \phi, t) \sim 16\pi \Re[\int r dr T_0^3 \varepsilon \delta T_1(r) \exp(-i\omega_1 t)]$. We interpret this frequency as the upper frequency component of the twin QPOs as argued earlier by LR07. Note that the higher order terms $\delta T_2, \delta T_3, \dots$ give no contribution to the total flux due to the ϕ -integration.

4.2. Driven Perturbations

Here we consider the driven perturbations of the flow which result from a quadrupole or octupole component of the star's magnetic field as discussed in §2.2. Inspection of equation (25) reveals that the radial locations of the Lindblad resonances where \mathcal{D} (or $\overline{\mathcal{D}}$) vanishes are very important for excitation of the flow (LR07). At such a

resonance the right-hand-side equation (25) - the driving term - is proportional to $\overline{\mathcal{D}}'(\overline{\mathcal{D}})^{-3/2}$.

We first consider the quadrupole field case B^{v1} where $m = 1$ for $\nu_r = \omega_r/2\pi = 300$ Hz and $\omega_i = 0$. We find that $\overline{\mathcal{D}}$ goes through zero at one radius, $r_L = 4.07r_S$ for this case. Near this radius we find $\overline{\mathcal{D}} \approx a(x - bx^2)$, where $x \equiv (r - r_L)/r_L$ and $a, b > 0$ are constants. We are interested as explained below to determine the amplitude of this driven mode near the vicinity of the corotation mode at $r_R = 3.92r_S$. For this purpose we develop an approximate solution to equation (25) for $x^2 \ll 1$ by retaining only the most singular term in the effective potential which is $U \approx (3/4)(\overline{\mathcal{D}}'/\overline{\mathcal{D}})^2$. The right-hand side of the equation can be approximated as $K\overline{\mathcal{D}}'(\overline{\mathcal{D}})^{-3/2}$, where $K \propto B^{v1}$. Thus equation (25) simplifies to

$$\frac{d^2\varphi}{dx^2} - \kappa^2\varphi = \frac{K(1 - 2bx)}{(x - bx^2)^{3/2}}, \quad (37)$$

where $\kappa^2 = (3/4)[(1 - 2bx)/(x - bx^2)]^2$. The inhomogeneous solution to this equation for $x^2 \ll 1$ is

$$\varphi = \frac{K}{3\sqrt{x}}. \quad (38)$$

Although φ diverges at $x = 0$, note that $\Psi = \delta p_*/\rho$ is a constant. For $-x$ increasing we find that the dependence of κ^2 changes from $\sim (3/4)x^{-2}$ to $\kappa^2 = \kappa_0^2 \approx 38$. The small value of κ_0^2 means that driven mode has a significant amplitude at the distance r_R where the free mode is excited.

With both the free perturbation and the quadrupole driven perturbation present we have

$$T(r, \phi, t) = T_0 + \Re[\delta T_1^f(r) \exp(i\phi - i\omega_1 t) + \delta T_1^d(r) \exp(i\phi - i\Omega_* t)]. \quad (39)$$

The associated flux density $S \sim T^4$ is

$$T_0^4 + 4T_0^3\Re[\delta T_1^f \exp(i\phi - i\omega_1 t) + \delta T_1^d \exp(i\phi - i\Omega_* t)] + 6T_0^2\Re\{\delta T_1^f \delta T_1^{d*} \exp[-i(\omega_1 - \Omega_*)t]\} + \dots, \quad (40)$$

where the ellipsis denotes terms of the form $\mathcal{O}[\exp(\pm 2i\phi)]$ and $\mathcal{O}[\exp(\pm 4i\phi)]$ which do not cause variations in the total flux. It follows from this equation that there are three QPO components for a generally oriented disk. Two of the components arise from the above-mentioned Doppler boost acting first on the term $\delta T_1^f \exp(i\phi - i\omega_1 t)$, which gives a frequency ω_1 component in the total flux, and second on the term $\delta T_1^d \exp(i\phi - i\Omega_* t)$, which gives a frequency Ω_* (the star's rotation frequency) in the total flux. The third component arises for the final term in equation (37) and has a frequency $\omega_1 - \Omega_*$. The component at Ω_* is however usually absent (van der Klis 2006) so that we do not consider this case further.

For the case of an octupole field component B^{v2} where $m = 2$ we find two Lindblad resonances for $\omega_r/2\pi = \Omega_*/2\pi = 300$ Hz and $\omega_i = 0$ as shown in Figure 7. One resonance is at $r_{Li}/r_S = 4.11$ and the other at $r_{Lo}/r_S = 4.28$. The driven motion at r_{Li} is important here because this is close to the radius of the unstable free perturbation r_R . For this case

$$T(r, \phi, t) = T_0 + \Re[\delta T_1^f(r) \exp(i\phi - i\omega_1 t) + \delta T_2^d(r) \exp(2i\phi - i\Omega_* t)]. \quad (41)$$

The associated flux density is

$$T_0^4 + 4T_0^3\Re[\delta T_1^f \exp(i\phi - i\omega_1 t) + \delta T_2^d \exp(2i\phi - i\Omega_* t)] + 6T_0^2\Re\{\delta T_1^f \delta T_2^{d*} \exp[-i\phi - i(\omega_1 - \Omega_*)t]\} + \dots \quad (42)$$

In this case we have just two frequency components: The first is at the frequency ω_1 of the unstable free perturbation as a result of the Doppler boost acting on the term $\delta T_1^f \exp(i\phi - i\omega_1 t)$. The second is at the frequency $\omega_1 - \Omega_*$ as a result of the Doppler boost acting on the term $\delta T_1^f \delta T_2^{d*} \exp[-i\phi - i(\omega_1 - \Omega_*)t]$. The Doppler boost acting on the remaining term in equation (39), $\delta T_2^d \exp(2i\phi - i\Omega_* t)$, causes no variation in the total flux.

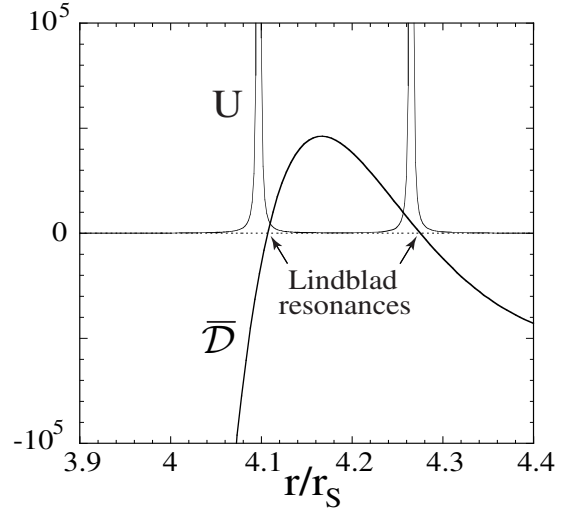


FIG. 7.— Radial dependence of the Lindblad factor $\overline{\mathcal{D}}$ (arbitrary scale) and the effective potential U (multiplied by r_S^2) for $\omega_r/2\pi = 300$ Hz, $\omega_i = 0$, and $m = 2$ and other conditions the same as in Figure 5.

4.3. Driven Modulated Perturbations

Here we consider the driven modulated perturbations of the flow which result from the octupole component of the star's magnetic field B^{v2} discussed in §2.3. Two Lindblad resonances are again found at radii similar to the case of Figure 7. The inner radius r_{Li} is important here because it is close to the radius r_R of the unstable free perturbation. For the driven modulated octupole case we have

$$T(r, \phi, t) = T_0 + \Re\{\delta T_1^f(r) \exp(i\phi - i\omega_1 t) + \delta T_2^{dm}(r) \exp[2i\phi - i(\Omega_*/2)t]\}. \quad (43)$$

The associated flux density is

$$T_0^4 + 4T_0^3\Re\{\delta T_1^f \exp(i\phi - i\omega_1 t) + \delta T_2^{dm} \exp[2i\phi - i(\Omega_*/2)t]\} + 6T_0^2\Re\{\delta T_1^f \delta T_2^{dm*} \exp[-i\phi - i(\omega_1 - \Omega_*/2)t]\} + \dots \quad (44)$$

In this case we again have just two frequency components: The first is at the frequency ω_1 of the unstable free perturbation as a result of the Doppler boost acting on the term $\delta T_1^f \exp(i\phi - i\omega_1 t)$. The second is at the frequency $\omega_1 - \Omega_*/2$ as a result of the Doppler boost acting on the term $\delta T_1^f \delta T_2^{dm*} \exp[-i\phi - i(\omega_1 - \Omega_*/2)t]$. The Doppler boost acting on the remaining term in equation (39), $\delta T_2^{dm} \exp[2i\phi - i(\Omega_*/2)t]$, causes no variation in the total flux. As mentioned in §2.3 the present theory does not predict the value of δT_2^{dm} .

5. NONLINEAR EFFECT OF UNSTABLE WAVE

The considered equilibrium disk (§3) does not include accretion. However, the unstable Rossby mode discussed in §4.1 gives rise to accretion in the vicinity of r_R ,

$$\dot{M}_{\text{Ro}} = -2\pi r \int_{-h}^h dz \Re(\delta\rho\delta u_r^*), \quad (45a)$$

where h is the half-thickness of the disk. We evaluate this by taking the most singular terms in $\Delta\omega$ in the limit where this quantity almost vanishes at $r = r_R$. This gives $\delta\rho = 2k_\phi \mathcal{F}\Psi/(\Delta\omega L_*)$, and $\delta u_r = -2ik_\phi \mathcal{F}\Psi/\rho$. Thus,

$$\dot{M}_{\text{Ro}} = -\frac{8\omega_i h k_\phi^2 |\mathcal{F}|^2 |\Psi|^2}{\rho |\Delta\omega|^2 L_*}, \quad (45b)$$

where $\omega_i > 0$ is the growth rate and $L_* < 0$. Thus, the instability acts increase the mass accretion rate, $\dot{M}_{\text{Ro}} > 0$.

The unstable Rossby mode also gives an inflow of angular momentum,

$$F_{\text{Ro}} = -2\pi r \int_{-h}^h dz \left[\Re(\delta\rho\delta u_r^*) r u_\phi + \rho \Re(\delta u_r^* r \delta u_\phi) \right]. \quad (46a)$$

Using the fact that $\rho\delta u_\phi = -k_\phi \mathcal{F}\Psi p'_*/(\rho\Omega_\phi \Delta\omega L_*)$, we find

$$F_{\text{Ro}} = \dot{M}_{\text{Ro}} \ell Q, \quad (46b)$$

where $Q = (1 + u_K^2/u_\phi^2)/2$ and $u_K = r\Omega_K$ is the Keplerian velocity. For the case of Figure 6, $Q = 1.884$. Because $Q > 1$, the Rossby mode transports inward more specific angular momentum ℓ than exists in the equilibrium. Consequently, a nonlinear effect of the Rossby mode is to make the positive slope of $\ell(r)$ smaller in the vicinity of r_R . A sufficiently large reduction of $d\ell/dr$ may cause the growth rate to decrease.

6. CONCLUSIONS

We have investigated three modes of accretion disks around rotating magnetized neutron stars which may explain the separations of the kilo-Hertz quasi-periodic oscillations (QPO) seen in low mass X-ray binaries. This work is a continuation of the earlier work by LR07 where these modes were identified. We develop the theory of compressible, non-barotropic MHD perturbations of an axisymmetric equilibrium flow with $\partial/\partial z = 0$. We assume that there is a maximum in the angular velocity $\Omega_\phi(r)$ of the accreting material larger than the angular velocity of the star Ω_* , and that the fluid is in approximately circular motion near this maximum rather than moving rapidly towards the star or out of the disk plane into funnel flows. MHD simulations by Romanova et al. (2002, 2008), Long et al. (2005), and Kulkarni & Romanova (2008) show this type of flow and $\Omega_\phi(r)$ profile.

The first mode we find is a Rossby wave instability or unstable corotation mode which is radially trapped in the vicinity of the maximum of a key function $g(r)\mathcal{F}(r)$ at r_R . We derive a Schrödinger type equation for the perturbation, $\varphi'' = U(r)\varphi$, where $U(r)$ is the effective potential. This instability is analogous to that found earlier by Lovelace & Hohlfield (1978), Lovelace et al. (1999), and

Li et al. (2000) and in simulations by Li et al. (2001). The real part of the angular frequency of the mode is $\omega_r = m\Omega_\phi(r_R)$, where $m = 1, 2, \dots$ is the azimuthal mode number. The imaginary part of the frequency ω_i (the growth rate) is determined by a Bohr-Sommerfeld quantization of the perturbation in the effective potential. We argue that for generally oriented disk, the Doppler boost of the disk surface emission from the unstable $m = 1$ mode will give periodic variations in the total flux with angular frequency ω_r which we suggest is the higher frequency component of the twin QPOs as proposed by LR07. The saturation of the growth of this mode remains to be analyzed in detail in future work.

The second mode, is a mode driven by the rotating, non-axisymmetric quadrupole [$\sim \exp(i\phi)$] and/or octupole [$\sim \exp(2i\phi)$] components of the star's magnetic field. It has an angular frequency equal to the star's angular rotation rate Ω_* . This mode is strongly excited near the radius of the Lindblad resonance which is slightly outside the radius of the maximum of $g\mathcal{F}$. When both the first and second modes are present the nonlinearity of the emission will in general give a product term with angular frequency $\omega_r - \Omega_*$. For a quadrupole field taking into account the Doppler boost, we find that the total flux has periodic variations at three frequencies, ω_r , Ω_* , and $\omega_r - \Omega_*$. However, the frequency Ω_* is usually not observed (van der Klis 2006). The situation is different for an octupole field component again taking into account the Doppler boost. In this case the total flux has periodic variations at two frequencies, ω_r the upper QPO and $\omega_r - \Omega_*$ the lower QPO.

The third mode arises from the interaction of the flow perturbation with the rotating non-axisymmetric components of the star's magnetic field. This interaction arises naturally owing to the fact that the magnetic force is proportional to the gradient of the square of the magnetic field. We derive a linear differential equation for this driven modulated perturbation. We find that the angular frequency of the perturbation is $\Omega_*/2$ both for the quadrupole and the octupole field components. In the case of the octupole field component and taking into account the Doppler boost, we find that the total flux has periodic variations at two frequencies, ω_r the upper QPO and $\omega_r - \Omega_*/2$ the lower QPO. Because the equation for the driven modulated perturbations is linear, the amplitude of the motion is indeterminate. One possibility is that the $\Omega_*/2$ motion is excited nonlinearly by the rotating non-axisymmetric field which has frequency Ω_* . This will be discussed in a future work. Thus present theory does not determine whether the lower QPO frequency is $\omega_r - \Omega_*$ or $\omega_r - \Omega_*/2$.

ACKNOWLEDGEMENTS

We thank Mr. Akshay Kulkarni and Prof. Chengmin Zhang for helpful comments. We thank the Maplesoft Technical Support Team for valuable assistance. The authors were supported in part by NASA grant NNX08AH25G and by NSF grants AST-0607135 and AST-0807129.

REFERENCES

- Alpar, M.A., & Psaltis, D. 2005, astro-ph/0511412
Balbus, S.A., & Hawley, J.F. 1998, *Rev. Mod. Phys.*, 70, 1
Fu, W., & Lai, D. 2009, *ApJ*, 690, 1386
Kato, S. 2004, *PASJ*, 56, 905
Koldoba, A.V., Romanova, M.M., Ustyugova, G.V., & Lovelace, R.V.E. 2002, *ApJ*, 576, L53
Kulkarni, A.K., & Romanova, M.M. 2008, *MNRAS*, 386, 673
Lamb, F.K., & Miller, M.C. 2001, *ApJ*, 554, 1210
Lamb, F.K., & Miller, M.C. 2003, astro-ph/0308179
Li, H., Finn, J.M., Lovelace, R.V.E., & Colgate, S.A. 2000, *ApJ*, 533, 1023
Li, H., Colgate, S.A., Wendroff, B., & Liska, R. 2001, *ApJ*, 551, 874
Li, L.-X., & Narayan, R. 2004, *ApJ*, 601, 414
Long, M., Romanova, M.M., & Lovelace, R.V.E. 2005, *ApJ*, 634, 1214
Lovelace, R.V.E., & Hohlfield, R.G. 1978, *ApJ*, 221, 51
Lovelace, R.V.E., Romanova, M.M., & Newman, W.I. 1994, *ApJ*, 437, 136
Lovelace, R.V.E., Li, H., Colgate, S.A., & Nelson, A.F. 1999, *ApJ*, 513, 805
Lovelace, R.V.E., & Romanova, M.M. 2007, *ApJ*, 670, L13 (LR07)
Miller, M.C., Lamb, F.K., & Psaltis, D. 1998, *ApJ*, 508, 791
Minorsky, N. 1974, *Nonlinear Oscillations*, (New York: Krieger Pub. Co.), p. 464
Romanova, M.M., Ustyugova, G.V., Koldoba, A.V., & Lovelace, R.V.E. 2002, *ApJ*, 578, 420
Romanova, M.M., Kulkarni, A.K., & Lovelace, R.V.E. 2008, *ApJ*, 673, L171
Sellwood, J.A., & Kahn, F.D. 1991, *MNRAS*, 250, 278
Shirakawa, A., & Lai, D. 2002, *ApJ*, 564, 361
Stella, L., & Vietri, M. 1999, *Phys. Rev. Lett.*, 82, 17
Tagger, M., & Varnière, P. 2006, *ApJ*, 652, 1457
Tagger, M., & Pellat, R. 1999, *A&A*, 349, 1003
van der Klis, M. 2006, in *Compact Stellar X-Ray Sources*, Eds. W.H.G. Lewin & M. van der Klis (Cambridge: Cambridge Univ. Press), p. 39
Zhang, C.M. 2004, *A&A*, 423, 401
Zhang, C.M., Yin, H.Z., Zhao, Y.H., Zhang, F., & Song, L.M. 2006, *MNRAS*, 366, 1373